Geophysical Research Letters

RESEARCH LETTER
10.1029/2018GL080172

Key Points:
- The aspect ratio of river basins is similar to that defined by triple divide junctions with neighboring basins
- An interdependency may exist between the basin's aspect ratio, the concavity of the river profile, and Hack's exponent
- The aspect ratio of river basins is sensitive to channel-forming processes as reflected by the concavity of the channel profile

Supporting Information:
- Supporting Information S1

Correspondence to:
E. Shelef,
shelef@pitt.edu

Citation:
Shelef, E. (2018). Channel profile and plan-view controls on the aspect ratio of river basins. *Geophysical Research Letters, 45*. https://doi.org/10.1029/2018GL080172

Received 23 AUG 2018
Accepted 23 OCT 2018
Accepted article online 25 OCT 2018

Channel Profile and Plan-View Controls on the Aspect Ratio of River Basins

Eitan Shelef[1]

[1]Department of Geological & Environmental Science, University of Pittsburgh, Pittsburgh, PA, USA

Abstract The ratio between the width and length (i.e., aspect ratio) of river basins is a fundamental attribute of Earth's surface. Topographic analyses showed that the aspect ratio of high-order basins along linear mountain fronts is surprisingly consistent despite different tectonic, lithologic, and climatic conditions. Additionally, analysis of simulated landscapes showed that the aspect ratio depends on the concavity of the river profile. These observations remain difficult to explain because of the intricate shape of river networks. Here I present a simple geometric model that computes the aspect ratio from the location of a triple divide junction with neighboring basins, the concavity of the river profile, and the exponent that relates river length and drainage area (i.e., Hack's exponent). The model suggests that these seemingly independent empirical observations are interdependent and that small basins that bound larger ones play a key role in determining the aspect ratio of the larger basins.

Plain Language Summary Despite the intricate geometry of river networks, their basins are characterized by a surprising regularity in the ratio between their width and length (i.e., aspect ratio). This regularity captures the pattern of landscape partitioning into river basins and hence the partitioning of water and life across Earth's surface. The causes for this regularity, however, remain unclear. This study presents a model that explains this regularity through the geometric configuration of adjacent river basins, as well as the geometry of the river profile. The agreement between model predictions and observations from natural and simulated landscapes suggests that small basins that bound larger ones play a key role in determining the aspect ratio of the larger basins and that the properties of the river profile (and hence of the erosive processes that carve this profile) are inherently linked to the aspect ratio of the river's basin.

1. Introduction

The structure of river networks portrays the spatial distribution of elevation, water, and life across Earth's surface and is also observed on other planets (e.g., Horton, 1945; Howard et al., 1994; Perron et al., 2006; Rinaldo et al., 1998; Sharp & Malin, 1975; Willett et al., 2014). Despite the intricate geometry of high-order channel networks, their basins are often characterized by a surprising regularity in the ratio (R) between the basin's width (W) and length (L; $R = W/L$; hereafter termed basin aspect ratio; Figure 1a; e.g., Bonnet, 2009; Castelltort & Simpson, 2006; Hovius, 1996; Talling et al., 1997). This ratio depicts the spacing between basin outlets (Hovius, 1996; Figure 1a) and thus the spacing and extent of depositional bodies that can form at these outlets. As such, it influences not only the shape of the landscape but also the extent and connectivity of water, oil, and gas that can accumulate in these depositional bodies (Hovius, 1996; Sømme et al., 2009; Talling et al., 1997).

The mean spacing between the outlets of large, high-order river basins ($\gtrsim 10^2$ km^2) along linear mountain fronts tends to be about half of the basins length (Hovius, 1996). This mean spacing is equivalent to the mean width of basins (supporting information S1 and Figure 1a) so the mean basin aspect ratio is approximately half. Observing this consistency, Hovius (1996) suggested that the basin width and drainage area (A) are related via a scaling law that is related to Hack's Law (Hack, 1957), an empirical power law that relates channel length to drainage area. However, the link between these two empirical relationships remained elusive.

The consistency in the aspect ratio of large basins is generally independent of climatic, lithologic, and tectonic conditions (Castelltort & Yamato, 2013; Hovius, 1996) and may reflect similarity in initial conditions (e.g., Castelltort & Yamato, 2013; Phillips & Schumm, 1987; Pelletier, 2003). Whereas the aspect ratio of small basins is sensitive to hydro-climatic factors, these factors do not meaningfully influence the aspect ratio of large basins ($\gtrsim 10^2$ km^2; Robert et al., 2018). The aspect ratio of large basins can however be influenced by initial

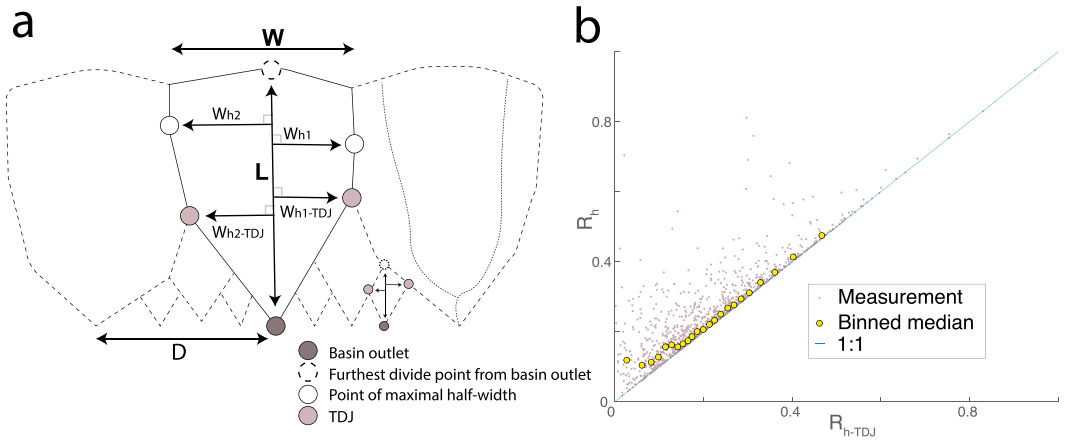

Figure 1. Channel spacing, aspect ratio, and TDJs (Triple Divide Junctions). (a) Schematic plan-view illustration of basins whose outlets are aligned. Dashed lines mark basin boundaries (i.e., divides), and a solid line marks the boundary of the analyzed basin. L is the length of the basin axis, W_h is the half width of the basin, W_{h-TDJ} is the TDJ-based half width, and subscripts 1 and 2 distinguish between the half widths in each side of the basin axis (note that $W = W_{h1} + W_{h2}$). Note that this geometry describes not only the large basins that reach the northern edge of the figure but also the smaller basins nested between them (e.g., see the outlet, head, and width marks on the nested basin at the lower right portion of this illustration). D is the distance between the outlets of large basins and is similar to the width of the basin (W; see supporting information S1 for details). The dotted lines in the rightmost basin mark two large channels that meet close to the outlet of the basin. (b) Relations between the half aspect ratio ($R_h = W_h/L$) and the TDJ-based half aspect ratio ($R_{h-TDJ} = W_{h-TDJ}/L$) measured for basins of different scales that drain to quasi-linear river valleys in the Loess Plateau, China. Each gray point marks a half aspect ratio measured for a specific basin ($N = 1,274$), and yellow circles mark binned median values that are binned such that each bin contains 50 measurements of half aspect ratio values. The diagonal line follows a 1:1 relation. Note that $R_h \geq R_{h-TDJ}$ and that the binned median values of R_h and R_{h-TDJ} are generally similar (i.e., $R_h \simeq R_{h-TDJ}$) where binned R_h values slightly exceed the binned R_{h-TDJ} values.

topographic conditions (e.g., Castelltort & Yamato, 2013; Phillips & Schumm, 1987; Pelletier, 2003), where narrower basins (i.e., low aspect ratio) develop when the roughness of the initial topography is low compared to the regional slope. Therefore, the consistency in aspect ratio may reflect a similarity in the initial topography formed early in the development of mountainous terrain where juvenile basins develop (Castelltort & Simpson, 2006; Castelltort et al., 2009; Castelltort & Yamato, 2013; Talling et al., 1997). Yet it remains unclear how and if the consistency in aspect ratio can be explained through the geometric relations between adjacent basins.

Numerical simulations suggest that basin's aspect ratio strongly covaries with the concavity of the channel profile. Sun et al. (1994) explored the synthetic topography produced by simulations of optimal channel networks (e.g., Rigon et al., 1993) and showed a strong covariance between the basin aspect ratio and the channel concavity (θ); an exponent value that describes the relations between channel slope and drainage area and is often interpreted as a reflection of the physical mechanism of different erosional processes (e.g., Seidl & Dietrich, 1992; Stock & Dietrich, 2006; Whipple & Tucker, 1999; Whipple et al., 2000). Similar association between concavity and basin aspect ratio was shown, yet not explicitly discussed, in synthetic landscapes produced by landscape evolution models (Howard, 1994; Tucker & Whipple, 2002). Whereas the channel concavity may influence the preservation of initial topographic conditions (Howard, 1994; Shelef & Hilley, 2014) and/or the topologic symmetry of channel networks (Shelef & Hilley, 2014), it is still unclear what causes the dependence of aspect ratio on channel concavity.

Despite the fundamental role of the basin aspect ratio in depicting Earth's topography, it remains unclear what geometric constraints govern this ratio, and why are these constraints independent of tectonic, lithology, and climate (i.e., Hovius, 1996). Further, whereas the spacing (and hence aspect ratio) of low-order channels was shown to reflect the relative magnitude of hillslope and channel-forming processes (i.e., Perron et al., 2009; 2012), the causes for the dependency between channel-forming processes, as captured by the channel concavity, and the aspect ratio of high-order basins (i.e., Sun et al., 1994) remain elusive. In this study, I address this knowledge gap through a geometric model that is based on the observation that the width of large basins is constrained by smaller basins in between them. The model successfully predicts observations from natural and synthetic landscapes, links the basin aspect ratio to the channel concavity, and corroborates

explanations regarding the independence of aspect ratio on tectonics, lithology, and climate. The model also finds an interdependency between some of the most fundamental empirical relations in geomorphology: the relations between river's length and drainage area (Hack's law), slope and drainage area (profile concavity, Flint's law, (Flint, 1974)), and basin's length and width (basin aspect ratio).

2. Method

2.1. Half Aspect Ratio

To capture the details of the basin geometry, I measured the half aspect ratio (R_h), a metric that describes the relative basin width at each side of the basin axis. The basin axis is defined as the line that connects the outlet of the basin to the point on the drainage divide that is furthest from the outlet (e.g., Rigon et al., 1996), and the axis length, L, is the length of this line (Figure 1a). The half-basin width, W_h, is the orthogonal distance between the basin's axis and the point furthest from it on one of its sides (Figure 1a). This width, divided by the length of the basin's axis, produces a basin's half aspect ratio ($R_h = W_h/L$), such that each basin is associated with two R_h values, one for each side of the basin's axis.

2.2. Basin Width Is Constrained by Intersections of Drainage Divides

Because the location of the furthest point from the basin axis (i.e., the point used to compute W_h, Figure 1a) is somewhat arbitrary, it is difficult to develop a simple prediction for the half aspect ratio. However, examination of natural and synthetic landscapes suggests that the width of a drainage basins is often similar to that determined by the location of a Triple Divide Junction (hereafter TDJ) between (a) the analyzed basin, (b) a neighboring basin of a similar scale, and (c) a third, smaller basin in between the aforementioned two basins (Figure 1a). The TDJ-based half width of a basin, W_{h-TDJ}, is measured in a similar way as the half-basin width, where the width is measured as the orthogonal distance between the basin's axis and the TDJ on a given side of the basin axis (Figure 1a). The associated TDJ-based half aspect ratios, R_{h-TDJ}, equals W_{h-TDJ}/L. Analysis of synthetic steady-state landscapes (i.e., when erosion and uplift are balanced everywhere across the landscape) produced with simulations of landscape evolution (supporting information S1), as well as of natural basins that drain to quasi-linear valleys in the Loess Plateau, China (Figure 1b), show that although R_h is larger than R_{h-TDJ} by definition, typical R_h values are similar, although slightly larger, than typical R_{h-TDJ} values (Figure 1b and supporting information S1). This general similarity between R_h and R_{h-TDJ} suggests that TDJs can be used to simplify the geometry of river basins and model their aspect ratio.

2.3. Geometric Model

The observation that basin's width is constrained by the TDJ guides a simple geometric model that ties the plan-view shape of a basin, the profile of fluvial channels, and the geometric configuration of adjacent basins. The model reduces the intricate plan-view geometry of a branched channel network to a simple configuration in which a single main channel, which is straight and orthogonal to a linear boundary (e.g., a mountain front), is joined by one tributary from each side (Figures 1a and 2a), where tributaries are orthogonal to the main channel. The upstream end of each tributary is a TDJ where the headwater of this tributary is also the headwater of a neighboring side channel that drains parallel to the main one toward the linear boundary (Figures 1a, 2a, and 2b). The elevation gain between the TDJ and the outlets of the main and side channels can thus be equated:

$$\Delta z_m + \Delta z_t + \Delta z_{ht} = \Delta z_s + \Delta z_{hs} + \Delta z_o, \tag{1}$$

where Δz is elevation gain along a channel section, and subscripts t, m, and s mark the tributary, main, and side channels, respectively (Figure 2b). Note that Δz_m marks the elevation gain along the section of the main channel, of length l_s, that is between the outlet and the junction with the tributary (Figures 1a, 2a, and 2b). Given that the TDJ is located at a hilltop, the hillslope relief between the TDJ and the head of the tributary and side channels is accounted for by Δz_{ht} and Δz_{hs}, respectively. Δz_o describes the elevation difference between the outlet of the side channel and that of the main channel.

For simplicity, I assume that for large basins, the hillslope length is negligible compared to the basin's width, that the hillslope relief is similar across the divide ($\Delta z_{ht}, \simeq \Delta z_{hs}$; e.g., Willett et al., 2014), and that the elevation difference between the outlets of the main and side channels is negligible compared to the elevation gained between the TDJ and the outlet of the main channel. In that case, and where Δz is substituted with the integration of slope along the channel length (l), equation (1) becomes

$$\int_0^{l_s} S_m(l)\,\mathrm{d}l + \int_0^{l_t} S_t(l)\,\mathrm{d}l = \int_0^{l_s} S_s(l)\,\mathrm{d}l, \tag{2}$$

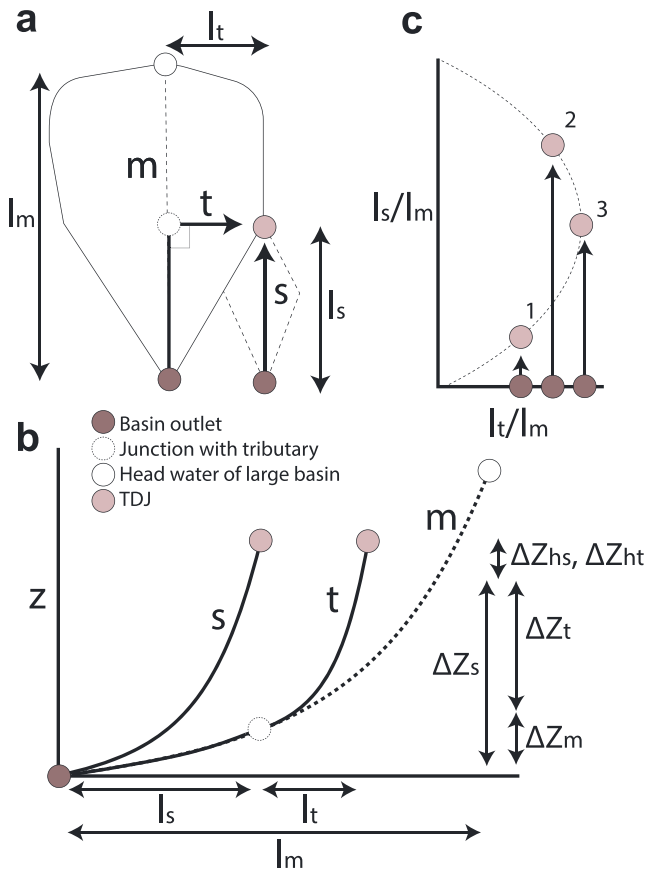

Figure 2. Geometric model. (a) Plan-view image of a modeled basin. The basin is drained by a straight main channel (marked *m*) and an orthogonal tributary (marked *t*), that is bounded by a TDJ (Triple Divide Junction) with a small neighboring channel (marked *s*, hereafter termed side channel) that flows parallel to the main channel. l_s, l_m, and l_t mark the length of each channel section and correspond to the bounds of integration in equations (2), (4), and to (6). (b) Profile view of the channels plotted in (a) where the outlets of the main and side channels are at the same elevation. ΔZ_m, ΔZ_t, ΔZ_s, ΔZ_{ht}, and ΔZ_{hs} correspond to equation (1). Note that the headwater of the tributary and that of the side channel are at the same elevation because they meet at the TDJ. (c) The normalized length of the tributary ($l_t/l_m = R_{h-TDJ}$) versus that of the side channel (l_s/l_m). In analysis of synthetic and natural landscape, l_s is represented by the distance between the outlet of the main basin and the point along the basin's axis that is orthogonal to the TDJ (e.g., Figure 1a), l_t is the orthogonal distance between the basin's axis and the TDJ, and l_m is the length of the basin's axis (i.e., $l_m = L$, so that $l_t/l_m = R_{h-TDJ}$). Note that such geometric model, where the TDJ constrains the basin's width, holds for channels at different scales (e.g., both the large and small channels in Figure 1).

where l_t, l_m, and l_s are the length of the tributary, main, and side channels, respectively, and l increases upstream (Figures 1, 2a, and 2b). When the landscape is at topographic steady state, the channel slope can be expressed in terms of its drainage area (A; Flint, 1974):

$$S(l) = K_s A^{-\theta}(l), \tag{3}$$

where θ is the aforementioned channel concavity, and K_s encapsulates the influence of tectonics, lithology, and climate on S (e.g., Whipple & Tucker, 1999; Wobus et al., 2006). For the case of a spatially uniform K_s, equation (3) can be substituted into equation (2) (Perron & Royden, 2012; Shelef & Hilley, 2014)

$$\int_0^{l_s} A_m^{-\theta}(l)\,\mathrm{d}l + \int_0^{l_t} A_t^{-\theta}(l)\,\mathrm{d}l = \int_0^{l_s} A_s^{-\theta}(l)\,\mathrm{d}l. \tag{4}$$

In the proposed geometric model, the TDJ-based half-basin width is similar to the length of the tributary, l_t (Figures 1, 2a, 2b) and can be computed from equation (4). The length of a channel can be expressed in terms of drainage area using Hack's (1957) law

$$A = k\lambda^h, \tag{5}$$

where k and h are Hack's coefficient and exponent, respectively, and λ is the channel length from the headwater (e.g., $\lambda_t = l_t - l$). Assuming that h, k, and θ are spatially uniform, equation (5) can be substituted into equation (4) and solved for l_t:

$$\begin{aligned} l_t &= [(l_m - l_s)^{1-\theta h} - l_m^{1-\theta h} + l_s^{1-\theta h}]^{1/(1-\theta h)},\ \theta h \neq 1, \\ l_t &= l_s(l_m - l_s),\ \theta h = 1. \end{aligned} \tag{6}$$

Note that l_t is independent of K_s and the climatic, lithologic, and tectonic influences that are encapsulated in it. In this model, l_t is akin to the TDJ-based half-width of a basin, and depends on the location of the TDJ along the main channel, as represented by the length of the main and side channels (l_m and l_s, respectively) in equation (6) (Figures 1 and 2). For example, when the side channel is relatively short so the elevation gain along its route to the TDJ is relatively small, a short tributary that initiates next to the outlet of the main channel suffices to produce the same elevation gain at the other side of the TDJ (case 1 in Figure 2c). When the length of the side channel is close to that of the main channel, so the gain in elevation along the two channels is similar, once again, a short tributary suffices to gain equality in elevation on both sides of the TDJ (case 2 in Figure 2c). The maximal tributary length occurs when the length of the side channel is half the length of the main channel (case 3 in Figure 2c and supporting information S1).

In contrast to the simple scenarios in Figure 2, where a basin gains width only through a tributary channel, the width of natural basins is also influenced by confluences (e.g., Robert et al., 2018). Channels upstream of a confluence, for example, can increase the width of a basin by diverging from the basin axis (e.g., see the channels [dotted line] in the rightmost basin in Figure 1a), and this divergence can be computed from the optimal angle between diverging channels at a confluence (e.g., Devauchelle et al., 2012; Howard, 1971; Hooshyar et al., 2017; Roy, 1983; Sólyom & Tucker, 2007; Seybold et al., 2017). For simplicity, the proposed model computes the width gained through such confluences (w_c [L]) based on a commonly used and relatively simple relation (Howard, 1971, 1990) and assumes that the basin width gained through multiple confluences along the channel can be represented by a single confluence between channels of similar drainage area (e.g., Robert et al., 2018).

$$w_c = c_c \sin\left[acos\left(\frac{S_b}{S_a}\right)\right] = c_c \sin\left[acos\left\{\left(\frac{A_b}{A_a}\right)^{-\theta}\right\}\right] = c_c \sin\left[acos\left(2^{-\theta}\right)\right], \quad (7)$$

where subscripts a and b mark the area and slope of the channels above and below the confluence, respectively, and c_c [L] is a scaling parameter.

To account for the width gained along the tributary and confluence (l_t and w_c, respectively), the TDJ-based half aspect ratio (R_{h-TDJ}) is computed by adding equations (6) and (7) and normalizing this total half-width by the length of the main channel (l_m, note that the model assumes $l_m = L$ and $W_{h-TDJ} = l_t + w_c$):

$$\begin{aligned} R_{h-TDJ} &= \frac{l_t + w_c}{l_m} \\ &= \left[(1 - \frac{l_s}{l_m})^{1-\theta h} - 1 + \frac{l_s}{l_m}^{1-\theta h}\right]^{1/(1-\theta h)} + \frac{c_c}{l_m} \sin\left[acos\left(2^{-\theta}\right)\right], \ \theta h \neq 1, \\ &= \frac{l_s}{l_m}(1 - \frac{l_s}{l_m}) + \frac{c_c}{l_m} \sin\left[acos\left(2^{-\theta}\right)\right], \ \theta h = 1. \end{aligned} \quad (8)$$

Given that R_{h-TDJ} (Figures 1 and 2) is a good proxy for the basin's half aspect ratio (R_h; Figure 1b and supporting information S1), the model predicts that the basin aspect ratio (i.e., $R = W/L \simeq 2R_{h-TDJ}$) depends on the channel concavity (θ), Hack's exponent (h), the location of the TDJ relative to the basin's axis, (l_s/l_m; Figure 2), and a parameter (c_c/l_m) that scales the influence of θ on the width gained through channel confluences. The model can thus be evaluated because all of these parameters, except for c_c/l_m, can be measured from topographic maps of natural or synthetic landscapes. Note that a zero concavity value ($\theta = 0$) results in $l_t = 0$ and $w_c = 0$, so that basins reduce to narrow lines that flow down a constant slope and are devoid of lateral flow convergence (i.e., in agreement with Smith & Bretherton, 1972).

2.4. Analysis of Synthetic and Natural Topography

The analytical model described above (equation (8)) suggests that the basin aspect ratio increases with channel concavity (assuming a constant Hack's exponent). Because high-order river basins in nature often deviate from model assumptions and have a narrow range of concavity values, I used a landscape evolution model (TTLEM; Campforts & Schwanghart, 2016) to simulate synthetic steady state landscapes for a wider range of concavity values (0.2 to 0.9) with a combination of the stream power law (e.g., Whipple & Tucker, 1999) and linear hillslope diffusion (Culling, 1963). The higher concavity values in this range exceed $\theta \simeq 0.7$, a value where the basin topology becomes relatively insensitive to the channel concavity (Shelef & Hilley, 2014). For simplicity, I used a slope exponent of $n = 1$ and varied the drainage area exponent m from 0.2 to 0.9 to form synthetic landscapes of different concavities (i.e., $\theta = m/n$). To conform to the assumption of relatively short hillslopes, I set the hillslope length in these simulations to be smaller than the distance between nodes (Perron et al., 2009; Shelef & Hilley, 2014). The initial topography was identical in all simulations and is composed of a flat surface with small-scale random noise. The dimensions of the simulated landscape were set to $20,000 \times 200$ nodes to produce a large number of basins in each simulation and enable robust statistical analyses.

To compare the proposed model (i.e., equation (8)) to natural and synthetic landscapes, the parameters (l_s, l_m, h, and θ) were automatically measured across these landscapes. For each basin, I first identified the basin's divide and axis and used them to measure R_h, R_{h-TDJ} (as defined in section 2.2 and Figures 1a and 2), the axis length (l_m), and the location of the TDJ orthogonal to the basin axis (l_s in the terminology of the geometric model in Figure 2). I used the length and drainage area of the channels to compute Hack's exponent (h). These measurements provided proxies for the model parameters (h, l_s, and l_m), where θ is prescribed in the simulations that form the synthetic landscapes and was measured for natural landscape using slope-area regression (e.g., Whipple & Tucker, 1999). This provides the variables needed to compare the model predictions of R_{h-TDJ} (equation (8)) with the R_{h-TDJ} and R_h values measured from synthetic and natural landscapes. The free parameter c_c/l_m (equation (8)) was set to a constant value which minimized the misfit between the modeled and measured R_{h-TDJ} and R_h at the central portion of basins (i.e., $0.3 < l_s/l_m < 0.7$) for all concavities up to $\theta = 0.7$ (i.e., the basin shape is relatively insensitive to θ when $\theta \gtrsim 0.7$; Shelef & Hilley, 2014). In the synthetic landscapes, the basin axis was computed from the outlet, at the boundary of this simulated landscape. For a natural example (i.e., Figure 1b and supporting information S1), I analyzed basins that drain to quasi-linear mountain fronts along river valleys in the Loess Plateau, China (supporting information S1), where the lithology and climate are generally homogeneous and the landscape is approximately at steady state (e.g., Willett et al., 2014). In that case, the channel outlet is the confluence between the measured basin and the quasi-linear river valley.

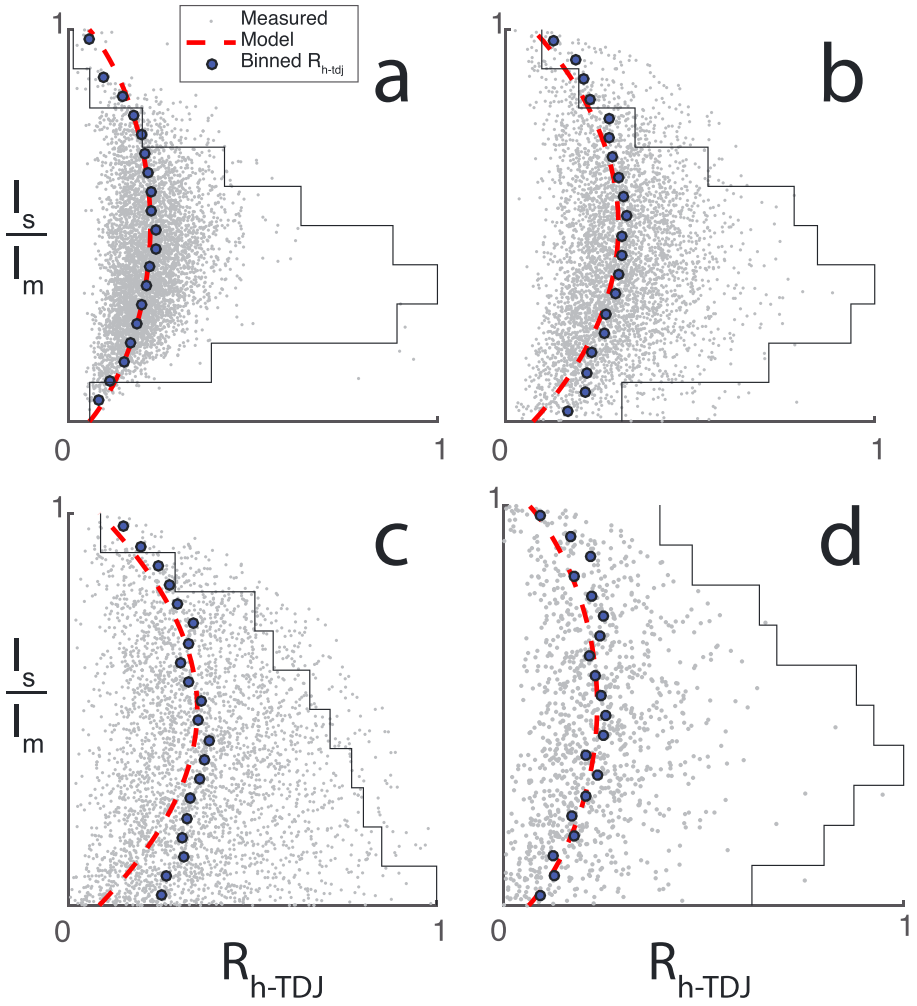

Figure 3. Model predictions versus measurements of l_s/l_m and R_{h-TDJ}. (a–c) Analysis of synthetic landscapes with concavity values of 0.25 (a), 0.5 (b), and 0.75 (c). (d) Analysis of basins in the Loess Plateau ($\theta \simeq 0.3$ and $h \simeq 1.7$). Gray dots show measured values of l_s/l_m and R_{h-TDJ}; blue circles mark median values of R_{h-TDJ} binned by l_s/l_m. Red-dashed line shows the prediction of the geometric model (equation (8)) of R_{h-TDJ} for $c_c/l_m = 0.11$ and varying l_s/l_m, where θ and h are the measured values associated with each of these landscapes. Measurements were conducted for all basins with $l_m > 10$ nodes for synthetic landscapes (a–c) and $l_m > 1,200$ m for the Loess Plateau (d). Dark stair-plot portrays a normalized histogram of the number of TDJs (Triple Divide Junctions) binned by l_s/l_m values; note that most of the TDJs are orthogonal to the central portion of the basin axis (i.e., $0.3 < l_s/l_m < 0.7$).

3. Results

The proposed model predicts that the TDJ-based half aspect ratio (R_{h-TDJ}) varies with the location of the TDJ relative to the main channel (l_s/l_m, Figure 2, equation (8)), as well as with the channel concavity and Hack's exponent (i.e., θ, h). For the synthetic landscapes that were used to produce basins with a wide range of θ values, the variations in Hack's exponent are relatively low (h has a coefficient of variation of ~5% across all concavities), so the variations in θh (equation (8)) are governed by the concavity. In synthetic landscapes of low concavity, the model predictions regarding variations in R_{h-TDJ} as a function of the TDJ location along the main channel (l_s/l_m) agree well with the median of the measured R_{h-TDJ} values (Figure 3). Measurements from the Loess Plateau ($\theta \simeq 0.3$) follow a similar trend (Figure 3d) and also show that the relative difference between measured R_h and R_{h-TDJ} values is typically about 5% regardless of basin size (supporting information S1) and that larger deviations between measured R_h and R_{h-TDJ} occur primarily where l_s/l_m values are <0.3 or >0.8 (supporting information S1). For synthetic landscapes of high concavity values, the median R_{h-TDJ} is typically higher than the values predicted by the model when the TDJ is located close to the head and outlet of the basin (i.e., $l_s/l_m = 1$, $l_s/l_m = 0$, respectively; Figure 3c). At the central portion of the synthetic basins

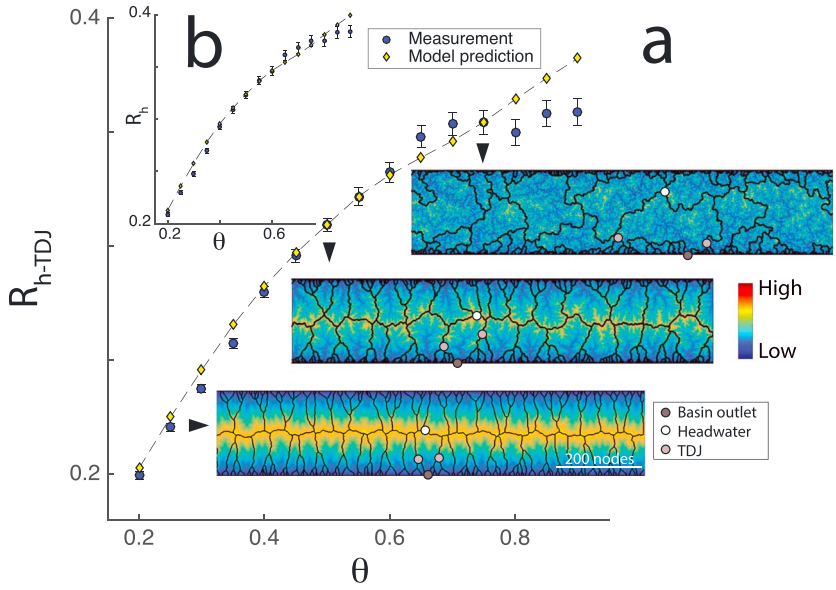

Figure 4. The influence of channel concavity on R_{h-TDJ} and R_h. (a) Values of R_{h-TDJ} computed from the geometric model (equation (8), green diamonds) versus those measured from synthetic landscapes of different channel concavities (blue circles, error bars mark the standard error of the median). The modeled R_{h-TDJ} values are computed by equation (8) at $l_s/l_m = 0.5$, with the θ and h values associated with each of the analyzed landscapes and with $c_c/l_m = 0.11$. The measured R_{h-TDJ} values are the median values of all R_{h-TDJ} located orthogonal to the central portion of the basin ($0.3 < l_s/l_m < 0.7$). The model produces an R^2 of 0.98 for concavities $\leq$0.7. Inset maps show the topographic elevation of sections of the synthetic landscapes (for concavity of 0.25, 0.5, and 0.75) that were used to measure l_s/l_m, h, R_{h-TDJ}, and R_h. The divides of basins used for the analysis are marked in black, and small circles show examples of basin outlet, headwater (i.e., furthest point on divide) and TDJs (Triple Divide Junction). (b) Same as (a), where now the modeled values are compared to the median values of R_h rather than to R_{h-TDJ}. This also produces an R^2 of 0.98 for concavities $\leq$ 0.7 ($c_c/l_m = 0.13$). Note that R_{h-TDJ} and R_h values at concavities close of 0.3–0.5 produce basin aspect ratios (i.e., $R \simeq 2R_h \simeq 2R_{h-TDJ}$) of about one half, in accordance with the typical values measured in natural landscapes (e.g., Hovius, 1996). Also note that measured R_{h-TDJ} and R_h values become relatively insensitive to θ for $\theta \gtrsim 0.7$.

(i.e., $0.3 < l_s/l_m < 0.7$), where most of the TDJs are located (Figure 3), the measured R_{h-TDJ} agrees well with the model prediction ($R^2 = 0.98$; Figure 4a) for concavity values $\lesssim 0.7$ with a $c_c/l_m = 0.11$. Similar agreement ($R^2 = 0.98$ for $0.3 < l_s/l_m < 0.7$; Figure 4b) exists between R_h and model prediction with a somewhat higher value of $c_c/l_m = 0.13$, in accordance with the slightly higher values of W_h compared to W_{h-TDJ} (Figure 1 and supporting information S1).

4. Discussion

The agreement between the modeled and measured values of R_{h-TDJ} varies with channel concavity and with the location of the TDJ along the basin axis (l_s/l_m, Figures 3 and 4). Low concavity networks at steady state typically have a simple geometry, where basin divides are constrained by a high symmetry in flow length between divides and outlets (Shelef & Hilley, 2014). This typically forms a simple basin geometry, similar to that of the proposed model (Figure 2), where side tributaries join a single trunk channel (Figure 4a) that is orthogonal to the mountain front. This is consistent with the close agreement between R_{h-TDJ} predicted by the model for different l_s/l_m values and that measured from synthetic landscapes of low concavity (Figure 3). In contrast, networks of high concavity are less restricted by symmetry of flow length (Shelef & Hilley, 2014) and are characterized by a contorted geometry with several large branches. These networks tend to deviate from the simple geometry of the model and generally preserve the network configuration imposed by the initial topography over which the networks evolve (Howard, 1994; Shelef & Hilley, 2014). The preservation of this initial network configuration is almost perfect at concavity values higher than ~0.7 (Shelef & Hilley, 2014), so the aspect ratio becomes relatively insensitive to concavity and deviates from model predictions (Figures 3 and 4). Such deviations are particularly common next to the basin outlet (or headwater) because of large confluences at these locations, and/or basin axis that is diagonal to the linear mountain front, and/or a relative narrowing of the basin width (i.e., Figure 2c) that meaningfully violates of the assumption that the hillslope

length is negligible relative to the basin width (i.e., equation (2)). In the analyzed landscapes, most of the TDJs are located close to the center of the basin axis (i.e., $0.3 < l_s/l_m < 0.7$; Figure 3 and supporting information S1) which is where model predictions are good for all concavities up to 0.7 (Figure 4; $R^2 = 0.98$). Further, natural concavity values are typically within the range where model predictions are good (i.e., $\theta < 0.7$; Tucker & Whipple, 2002, Whipple & Tucker, 1999); hence, the proposed model generally provides a good prediction for R_{h-TDJ} and R_h for concavity and l_s/l_m values that are common in nature, and may thus link the aspect ratio to natural channel-forming processes as reflected by the channel concavity (θ).

The proposed model is based on the assumption that the landscape is in steady-state and that lithology and climate are spatially constant. This is aligned with the general match between model predictions and the aspect ratios measured in the Loess Plateau (Figure 3d), where these assumptions are generally met (e.g., Willett et al., 2014). However, the model predictions, based on h and θ values that are common in nature (i.e., $h \simeq 1.7$, $0.3 \lesssim \theta \lesssim 0.7$; Rigon et al., 1996; Tucker & Whipple, 2002; Whipple & Tucker, 1999), also agree with aspect ratio values measured along linear mountain fronts (Hovius, 1996; i.e., $R = W/L \simeq 2R_h \simeq 2R_{h-TDJ}$), where the model assumptions are likely violated because of heterogeneous uplift rates, lithology, and climate. It is therefore possible that these natural heterogeneities do not suffice to substantially influences the basin aspect ratio. Future studies can likely utilize the proposed model to explore the sensitivity of aspect ratio to spatial heterogeneities in tectonic, lithology, and climate.

The model connects seemingly independent empirical observations (i.e., aspect ratio, Hack's exponent, and channel concavity) and, in doing so, formulates an interdependency between three prominent topographic consistencies. Whereas this study primarily explores the dependence between θ and the basin aspect ratio, future studies may reveal other implications of this interdependency.

Whereas the proposed model generally predicts the relations between basin aspect ratio and channel concavity, important questions regarding the geometry of basins in diverse settings are yet to be addressed. For example, the geometry of the model describes a simple case where basins are perpendicular to a linear boundary of uniform elevation, and it is unclear whether the proposed TDJ-based approach holds for geometric settings that meaningfully deviate from this simple scenario. The relations between R_h and R_{h-TDJ} and their response to tectonic and/or climatic perturbations are also worthy of further exploration. Further, whereas the value of R_{h-TDJ} is sensitive to the relative location of the TDJ (i.e., l_s/l_m), this study does not explore potential controls on and influences of this relative location: whether it is sensitive to tectonic and climatic conditions, how does it influence the topography of ridge lines (i.e., Spotila, 2012), and how does it change through the temporal evolution of landscapes (e.g., Densmore et al., 2005; Frankel & Pazzaglia, 2006). Although this study does not explicitly address these questions, the proposed TDJ-based approach can be utilized to explore them. This can be done by adjusting the model's bounds of integration and/or angular relations to different geometric settings or by exploring the influence of perturbations (i.e., geomorphic, tectonic, climatic) on the relative location of the TDJ, and on the relations between R_h and R_{h-TDJ}.

5. Summary

This research presents a simple geometric model aimed to explain the consistency in basin's aspect ratio along linear mountain fronts and the dependence of aspect ratio on channel concavity. The model is based on the similarity between the maximal width of the basin and the width determined by the TDJ between the divides of the analyzed basin, a neighboring basin of similar scale, and a third, smaller basin in between the aforementioned two basins. Measurements of synthetic and natural landscapes generally agree with model prediction and show that the TDJ-based aspect ratio is sensitive to the channel concavity (θ). The accuracy of model predictions regarding the sensitivity of the TDJ-based basin width to the location of the TDJ varies with channel concavity, yet, when the TDJ is orthogonal to the central portion of the basin axis, the model predictions are good for concavity values $\lesssim$0.7, in accordance with prior studies that showed that the shape of river networks is relatively insensitive to concavity values $\gtrsim$0.7. These findings suggest that the basin aspect ratio is generally sensitive to channel-forming processes as reflected by the channel concavity and that small basins that bound larger ones play a key role in determining the aspect ratio of the larger basins. The model is also consistent with the observed independence of the basin's aspect ratio on tectonic, lithology, and climate. Finally, the model proposes that the basin's aspect ratio, Hack's exponent, and channel concavity are interdependent and will hopefully prompt exploration of deeper connections between these oft-used and seemingly independent empirical measures.

Acknowledgments
Data that were used in the analysis are contained in figures within the manuscript and supplements and the DEMs that were used in this study are publicly available. I thank Dr. George Hilley for valuable discussions regarding the influence of channel concavity on basin geometry, to Dr. Liran Goren, Dr. Sam Johnstone, Taylor Rohan, and Nick Wondolowsky for insightful comments on an early version of this manuscript, and to Dr. Benjamin Campforts for TTLEM support. I also thank Dr. Bayani Cardenas and two anonymous reviewers for constructive and thoughtful comments that helped improve this manuscript.

References

Bonnet, S. (2009). Shrinking and splitting of drainage basins in orogenic landscapes from the migration of the main drainage divide. *Nature Geoscience*, *2*(11), 766–771. https://doi.org/10.1038/ngeo666

Campforts, B., & Schwanghart, W. (2016). TTLEM — An implicit-explicit (IMEX) scheme for modelling landscape evolution in MATLAB. In *EGU General Assembly Conference Abstracts* (14137 pp.).

Castelltort, S., & Simpson, G. (2006). River spacing and drainage network growth in widening mountain ranges. *Basin Research*, *18*(3), 267–276. https://doi.org/10.1111/j.365-2117.2006.00293.x

Castelltort, S., Simpson, G., & Darrioulat, A. (2009). Slope-control on the aspect ratio of river basins. *Terra Nova*, *21*(4), 265–270. https://doi.org/10.1111/j.1365-3121.2009.00880.x

Castelltort, S., & Yamato, P. (2013). The influence of surface slope on the shape of river basins: Comparison between nature and numerical landscape simulations. *Geomorphology*, *192*, 71–79. https://doi.org/10.1016/j.geomorph.2013.03.022

Culling, W. (1963). Soil creep and the development of hillside slopes. *The Journal of Geology*, *71*(2), 127–161.

Densmore, A. L., Dawers, N. H., Gupta, S., & Guidon, R. (2005). What sets topographic relief in extensional footwalls? *Geology*, *33*(6), 453–456. https://doi.org/10.1130/G21440.1

Devauchelle, O., Petroff, A., Seybold, H., & Rothman, D. (2012). Ramification of stream networks. *Proceedings of the National Academy of Sciences*, *109*(51), 20,832–20,836. https://doi.org/10.1073/pnas.1215218109

Flint, J. (1974). Stream gradient as a function of order, magnitude, and discharge. *Water Resources Research*, *10*(5), 969–973. https://doi.org/10.1029/WR010i005p00969

Frankel, K. L., & Pazzaglia, F. J. (2006). Mountain fronts, base-level fall, and landscape evolution: Insights from the southern Rocky Mountains. *Special Papers-Geological Society of America*, *398*, 419. https://doi.org/10.1130/2006.2398(26)

Hack, J. (1957). Studies of longitudinal stream profiles in Virginia and Maryland. *United States Geological Survey Professional Paper*, *292*, 45–97.

Hooshyar, M., Singh, A., & Wang, D. (2017). Hydrologic controls on junction angle of river networks. *Water Resources Research*, *53*, 4073–4083. https://doi.org/10.1002/2016WR020267

Horton, R. (1945). Erosional development of streams and their drainage basins; hydrophysical approach to quantitative morphology. *Geological Society of America Bulletin*, *56*(3), 275–370.

Hovius, N. (1996). Regular spacing of drainage outlets from linear mountain belts. *Basin Research*, *8*(1), 29–44.

Howard, A. D. (1971). Optimal angles of stream junction: Geometric, stability to capture, and minimum power criteria. *Water Resources Philosophy and Phenomenological Research*, *7*(4), 863–873.

Howard, A. D. (1990). Theoretical model of optimal drainage networks. *Water Resources Research*, *26*(9), 2107–2117. https://doi.org/10.1029/WR026i009p02107

Howard, A. D. (1994). A detachment-limited model of drainage basin evolution. *Water resources research*, *30*(7), 2261–2285.

Howard, A. D., Dietrich, W. E., & Seidl, M. A. (1994). Modeling fluvial erosion on regional to continental scales. *Journal of Geophysical Research*, *99*(B7), 13,971–13,986.

Pelletier, J. D. (2003). Drainage basin evolution in the rainfall erosion facility: Dependence on initial conditions. *Geomorphology*, *53*(1-2), 183–196. https://doi.org/10.1016/S0169-555X(02)00353-7

Perron, J. T., Kirchner, J. W., & Dietrich, W. E. (2009). Formation of evenly spaced ridges and valleys. *Nature*, *460*(7254), 502–505. https://doi.org/10.1038/nature08174

Perron, J. T., Lamb, M. P., Koven, C. D., Fung, I. Y., Yager, E., & Ádámkovics, M. (2006). Valley formation and methane precipitation rates on Titan. *Journal of Geophysical Research*, *111*, E11001. https://doi.org/10.1029/2005JE002602

Perron, J., Richardson, P., Ferrier, K., & Lapôtre, M. (2012). The root of branching river networks. *Nature*, *492*(7427), 100–103. https://doi.org/10.1038/nature11672

Perron, J. T., & Royden, L. (2012). An integral approach to bedrock river profile analysis. *Earth Surface Processes and Landforms*, *38*, 570–576. https://doi.org/10.1002/esp.3302

Phillips, L. F., & Schumm, S. (1987). Effect of regional slope on drainage networks. *Geology*, *15*(9), 813–816.

Rigon, R., Rinaldo, A., Rodriguez-Iturbe, I., Bras, R. L., & Ijjasz-Vasquez, E. (1993). Optimal channel networks: A framework for the study of river basin morphology. *Water Resources Research*, *29*(6), 1635–1646.

Rigon, R., Rodriguez-Iturbe, I., Maritan, A., Giacometti, A., Tarboton, D. G., & Rinaldo, A. (1996). On Hack's law. *Water Resource Research*, *32*(11), 3367–3374. https://doi.org/10.1029/96WR02397

Rinaldo, A., Rodriguez-Iturbe, I., & Rigon, R. (1998). Channel networks. *Annual review of earth and planetary sciences*, *26*(1), 289–327. https://doi.org/10.1146/annurev.earth.26.1.289

Robert, S. Y., Arredondo, Á., Stansifer, E., Seybold, H., & Rothman, D. H. (2018). Shapes of river networks. *Proceedings of the Royal Society A*, *474*(2215), 20180081.

Roy, A. G. (1983). Optimal angular geometry models of river branching. *Geographical Analysis*, *15*(2), 87–96.

Seidl, M., & Dietrich, W. (1992). The problem of channel erosion into bedrock. In K. Schmidt, & J. de Ploey (Eds.), *Functional geomorphology: Landform analysis and models: Festschrift for Frank Ahnert, vol. Catena Supplement* (Vol. 23, pp. 101–124). Germany, Catena Verlag: Cremlingen.

Seybold, H., Rothman, D. H., & Kirchner, J. W. (2017). Climate's watermark in the geometry of stream networks. *Geophysical Research Letters*, *44*, 2272–2280. https://doi.org/10.1002/2016GL072089

Sharp, R. P., & Malin, M. C. (1975). Channels on Mars. *Geological Society of America Bulletin*, *86*(5), 593–609.

Shelef, E., & Hilley, G. E. (2014). Symmetry, randomness, and process in the structure of branched channel networks. *Geophysical Research Letters*, *41*, 3485–3493. https://doi.org/10.1002/2014GL059816

Smith, T. R., & Bretherton, F. P. (1972). Stability and the conservation of mass in drainage basin evolution. *Water Resources Research*, *8*(6), 1506–1529. https://doi.org/10.1029/WR008i006p01506

Sólyom, P. B., & Tucker, G. E. (2007). The importance of the catchment area–length relationship in governing non-steady state hydrology, optimal junction angles and drainage network pattern. *Geomorphology*, *88*(1-2), 84–108. https://doi.org/10.1016/j.geomorph.2006.10.014

Sømme, T. O., Helland-Hansen, W., Martinsen, O. J., & Thurmond, J. B. (2009). Relationships between morphological and sedimentological parameters in source-to-sink systems: A basis for predicting semi-quantitative characteristics in subsurface systems. *Basin Research*, *21*(4), 361–387. https://doi.org/10.1111/j.1365-2117.2009.00397.x

Spotila, J. A. (2012). Influence of drainage divide structure on the distribution of mountain peaks. *Geology*, *40*(9), 855–858. https://doi.org/10.1130/G33338.1

Stock, J. D., & Dietrich, W. E. (2006). Erosion of steepland valleys by debris flows. *Geological Society of America Bulletin*, *118*(9-10), 1125. https://doi.org/10.1130/B25902.1

Sun, T., Meakin, P., & Jøssang, T. (1994). The topography of optimal drainage basins. *Water Resources Research*, *30*(9), 2599–2610.

Talling, P. J., Stewart, M. D., Stark, C. P., Gupta, S., & Vincent, S. J. (1997). Regular spacing of drainage outlets from linear fault blocks. *Basin research*, *9*(4), 275–302.

Tucker, G., & Whipple, K. (2002). Topographic outcomes predicted by stream erosion models: Sensitivity analysis and intermodel comparison. *Journal of Geophysical Research*, *107*(B9), 2179. https://doi.org/10.1029/2001JB000162

Whipple, K. X., Hancock, G. S., & Anderson, R. S. (2000). River incision into bedrock: Mechanics and relative efficacy of plucking, abrasion, and cavitation. *Bulletin of the Geological Society of America*, *112*(3), 490–503. https://doi.org/10.1130/0016-7606(2000)112%3C490:RIIBMA%3E2.0.CO;2

Whipple, K., & Tucker, G. (1999). Dynamics of the stream-power river incision model: Implications for height limits of mountain ranges, landscape response timescales, and research needs. *Journal of Geophysical Research*, *104*(B8), 17,661–17,674. https://doi.org/10.1029/1999JB900120

Willett, S. D., McCoy, S. W., Perron, J. T., Goren, L., & Chen, C.-Y. (2014). Dynamic reorganization of river basins. *Science*, *343*(6175), 1248765. https://doi.org/10.1126/science.1248765

Wobus, C., Whipple, K. X., Kirby, E., Snyder, N., Johnson, J., Spyropolou, K., et al. (2006). Tectonics from topography: Procedures, promise, and pitfalls. *Special papers-geological society of america*, *398*, 55. https://doi.org/10.1130/2006.2398(04)